Retrospective prediction of the global warming slowdown in the past decade

Virginie Guemas[1,2]*, Francisco J. Doblas-Reyes[1,3], Isabel Andreu-Burillo[1] and Muhammad Asif[1]

Despite a sustained production of anthropogenic greenhouse gases, the Earth's mean near-surface temperature paused its rise during the 2000–2010 period[1]. To explain such a pause, an increase in ocean heat uptake below the superficial ocean layer[2,3] has been proposed to overcompensate for the Earth's heat storage. Contributions have also been suggested from the deep prolonged solar minimum[4], the stratospheric water vapour[5], the stratospheric[6] and tropospheric aerosols[7]. However, a robust attribution of this warming slowdown has not been achievable up to now. Here we show successful retrospective predictions of this warming slowdown up to 5 years ahead, the analysis of which allows us to attribute the onset of this slowdown to an increase in ocean heat uptake. Sensitivity experiments accounting only for the external radiative forcings do not reproduce the slowdown. The top-of-atmosphere net energy input remained in the [0.5–1] W m^{-2} interval during the past decade, which is successfully captured by our predictions. Most of this excess energy was absorbed in the top 700 m of the ocean at the onset of the warming pause, 65% of it in the tropical Pacific and Atlantic oceans. Our results hence point at the key role of the ocean heat uptake in the recent warming slowdown. The ability to predict retrospectively this slowdown not only strengthens our confidence in the robustness of our climate models, but also enhances the socio-economic relevance of operational decadal climate predictions.

The recent global warming slowdown despite the sustained top-of-atmosphere (TOA) excess energy input associated with the greenhouse gases triggered a debate on the fate of the missing heat[2–8]. A potential absorption of this heat by the atmosphere, the land or the sea ice has been ruled out using observational data sets[8]. Dissecting the internally generated variability in a climate model, this warming slowdown has been argued[2] to come partly from an increased radiation to space, associated with the El Niño/Southern Oscillation variability, and partly from increased deep-ocean warming, associated with the Atlantic meridional overturning circulation. An internal origin of this warming slowdown was suggested in another climate model[3], mostly related to a deep-ocean heat uptake associated with both the subtropical Pacific circulation and Atlantic meridional overturning circulation variability.

Near-term climate prediction[9–11] offers an optimal framework to test the hypotheses suggested in the literature to explain the observed twenty-first-century warming slowdown. At the edge between seasonal forecasting and climate-change projections, near-term climate predictions exploit the predictability of the climate system arising both from initializing the internal natural variability and from the changes in radiative external forcings[12], whereas climate projections benefit only from the latter. Successful retrospective predictions thus stand as an opportunity to attribute this warming slowdown to the interannual internal variability or the radiative external forcings, whereas observation analysis alone allows for detection and drawing of hypotheses but not for any attribution. The ability of the present generation of climate forecast systems to capture the pause in sea surface temperature (SST) rise from 2000 onward is not only crucial for adaptation but also a new challenge for climate modellers[1].

Such a challenge is taken up with the EC-Earth forecast system[13,14] in the Init experiment in which all of the model state variables are initialized from estimates of the observed climate state, namely from the ORAS4 reanalysis[15,16] for the ocean component, from the ERA40 reanalysis[17] for the atmosphere and land surface before 1989 and the ERAinterim[18] one afterwards, and from two different sources of sea-ice initial conditions (see Methods for further details). In those retrospective predictions initialized every November from 1960 to 2011, the ensemble-mean SST averaged over the first 3 forecast years (Fig. 1a) is very close to the observed 3-year running mean SST in all of the predictions from 2000 onward (one large dot per ensemble-mean prediction). The root mean square error (RMSE) computed from the ensemble-mean forecasts initialized between 2001 and 2005 is 0.027 K and spans the range [0.026–0.059] K for the individual ensemble members. On average over the forecast years 3–5, the warming slowdown is slightly less well captured with the RMSE reaching 0.052 [0.044–0.087] K (Fig. 1b). It is still however, much better captured than in the NoInit sensitivity experiment (in blue), which does not include any information about the previous history of the observed variability but only information about the radiative external forcing prescribed as in Init. The equivalent RMSE in NoInit is 0.100 [0.058–0.120] K (Fig. 1c). Initializing the EC-Earth forecast system from estimates of the observed climate state substantially improves its performance in predicting the global SST of the past decade. The computation of the 3-year SST tendency along each forecast provides further insight into the ability of the EC-Earth forecast system to capture the mechanism leading to such a warming slowdown. The 3-year mean SST changes (Fig. 1d) are computed as the difference between the 3-year mean SST after and before the year indicated in the x axis. The 3-year mean SST changes are better captured in Init than NoInit in the core of the warming slowdown, which means that the ability of EC-Earth to forecast the warming slowdown beyond 3 years does not come only from persistence of the initial conditions (also illustrated in Supplementary Fig. S1) but largely from its ability to capture the processes leading to

[1]Institut Català de Ciències del Clima (IC3), Doctor Trueta, 203, 08005 Barcelona, Spain, [2]Centre National de Recherches Météorologiques/Groupe d'Etude de l'Atmosphère Météorologique, Météo-France, CNRS, UMR 3589, Toulouse, France, [3]Instituciò Catalana de Recerca i Estudis Avançats (ICREA), Barcelona 08010, Spain. *e-mail: virginie.guemas@ic3.cat.
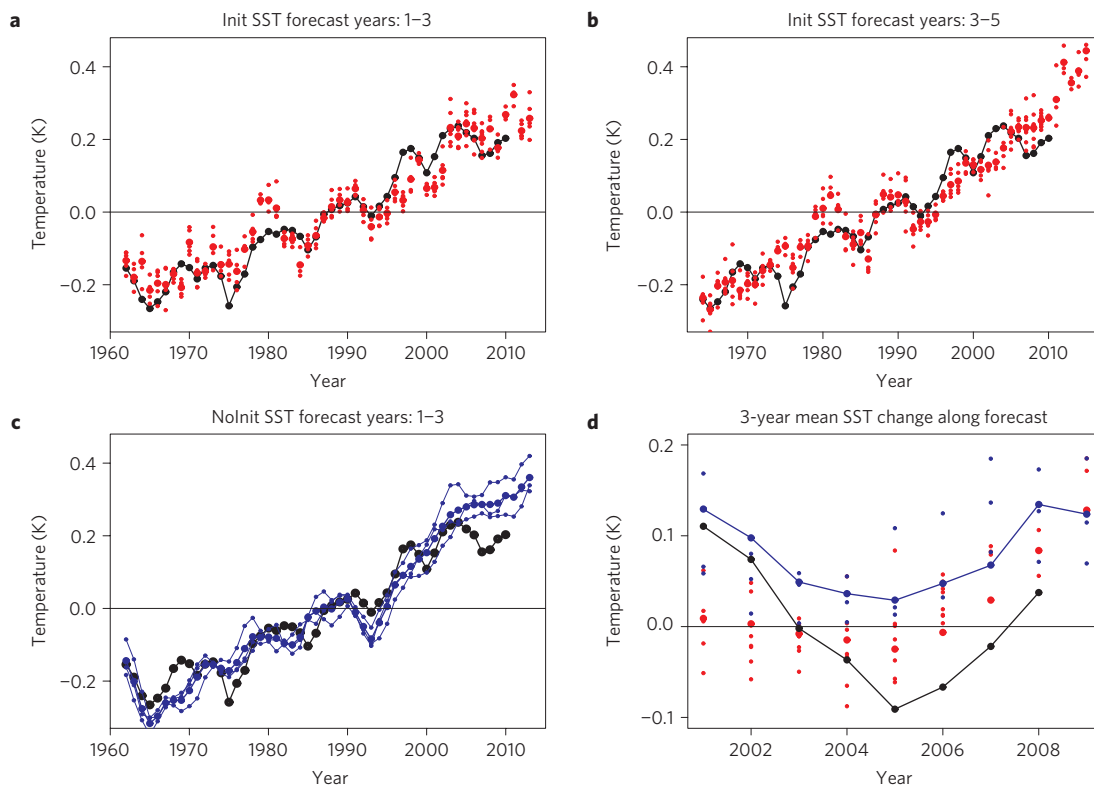
Figure 1 | Ability to capture the warming slowdown. a–c, Global SST anomalies averaged between 60° S and 65° N and across forecast years 1–3 (**a,c**) and forecast years 3–5 (**b**). **d**, 3-year mean SST change along the forecasts. One large dot is shown for the ensemble mean of each forecast and small dots are shown for their members in Init (red). The equivalents in NoInit and in the observations are shown in blue and black respectively, joined by lines as they come from a continuous time series.

the warming slowdown. Initializing the forecast system with the contemporaneous dynamical and thermodynamical climate system state seems crucial to capture the negative SST tendency, although this negative tendency is underestimated.

In spite of the warming slowdown, the observed CERES TOA net radiative flux remained positive (downward) during the early twenty-first century as shown in Fig. 2a in black. Both Init and NoInit reproduce this positive net TOA radiative flux and stand within the observational uncertainty estimated as 0.38 and 0.5 W m^{-2} in different studies[19,20]. Supplementary Fig. S2 shows that most of the TOA excess energy is absorbed by the ocean–sea ice system and Supplementary Fig. S3 illustrates that the contribution of the sea-ice system to this energy absorption amounts to about 1%, thus leaving the ocean as the main contributor. The negligible contributions from the atmosphere, land and sea ice are consistent with previous findings[8]. The 3-year accumulated global ocean heat uptake in the ORAS4 ocean reanalysis, computed as the difference between the 3-year mean total-column ocean heat content (OHC) after and before the year indicated in the x axis (Fig. 2b), is consistent with the TOA excess energy within the observational uncertainty. The ORAS4 ocean heat uptake shows a peak reaching about 0.55×10^{23} J at the beginning of the warming slowdown, which exceeds slightly the TOA excess energy at the same date, therefore accounting for the atmosphere and land surface cooling. The ORAS4 total OHC anomalies show consistently a sharp increase from 2000 (Fig. 3). The peak in ORAS4 ocean heat uptake around 2002 stands as the largest ocean heat uptake ever recorded over the whole observational period (Fig. 3d). The Init total OHC anomalies follow closely the ORAS4 ones until the third forecast year (Fig. 3a) and are still in reasonable agreement with ORAS4 until forecast year 5 (Fig. 3b) whereas NoInit OHC (Fig. 3c) barely exhibits any oscillation around the

long-term warming trend. The 3-year accumulated ocean heat uptake along the different forecasts in Init (in red, Figs 2b and 3d) illustrates that the peak is captured by EC-Earth and also stands as the largest peak in ocean heat uptake ever simulated by EC-Earth. Although underestimated, the ocean heat uptake is about 50% larger in Init than NoInit during the peak in the early warming slowdown (Fig. 2b). A proper initialization seems crucial to simulate the penetration of the heat into the ocean with the correct timing, and hence its impact on the global warming slowdown in the past decade.

The peak in total ocean heat uptake (Fig. 2b) is mostly explained by the upper (0–724 m) ocean (Fig. 2c) where the corresponding peak is captured by Init, but similarly underestimated as compared with ORAS4. Such a peak also appears in the best estimate of 0–700 m OHC available so far[21] shown with squares. The ocean mixed-layer heat content (Fig. 2d, triangles) exhibits a similar stabilization or slight decrease as the SST whereas the layer below (diamonds) is responsible for the peak. The decomposition per basin (Fig. 2e–g) highlights the tropical Pacific, the tropical Atlantic and the North Atlantic absorption below the mixed layer (diamonds) as the main contributors to this enhanced ocean heat uptake. Those basins explain 42%, 25% and 16% of the upper ocean heat uptake at the time of its maximum, respectively. Supplementary Fig. S4 illustrates the negligible contribution of other regions. The ocean heat uptake below the mixed layer exceeds slightly the TOA excess energy, therefore accounting for the observed cooling of the land, near-surface atmosphere and ocean superficial layer. Supplementary Fig. S5 provides further insight into the spatial distribution of the ocean heat uptake estimated from several observational data sets. Although occurring too early, the peak in tropical Pacific OHC absorption below the mixed layer is captured by Init with correct amplitude (Fig. 2e and Supplementary
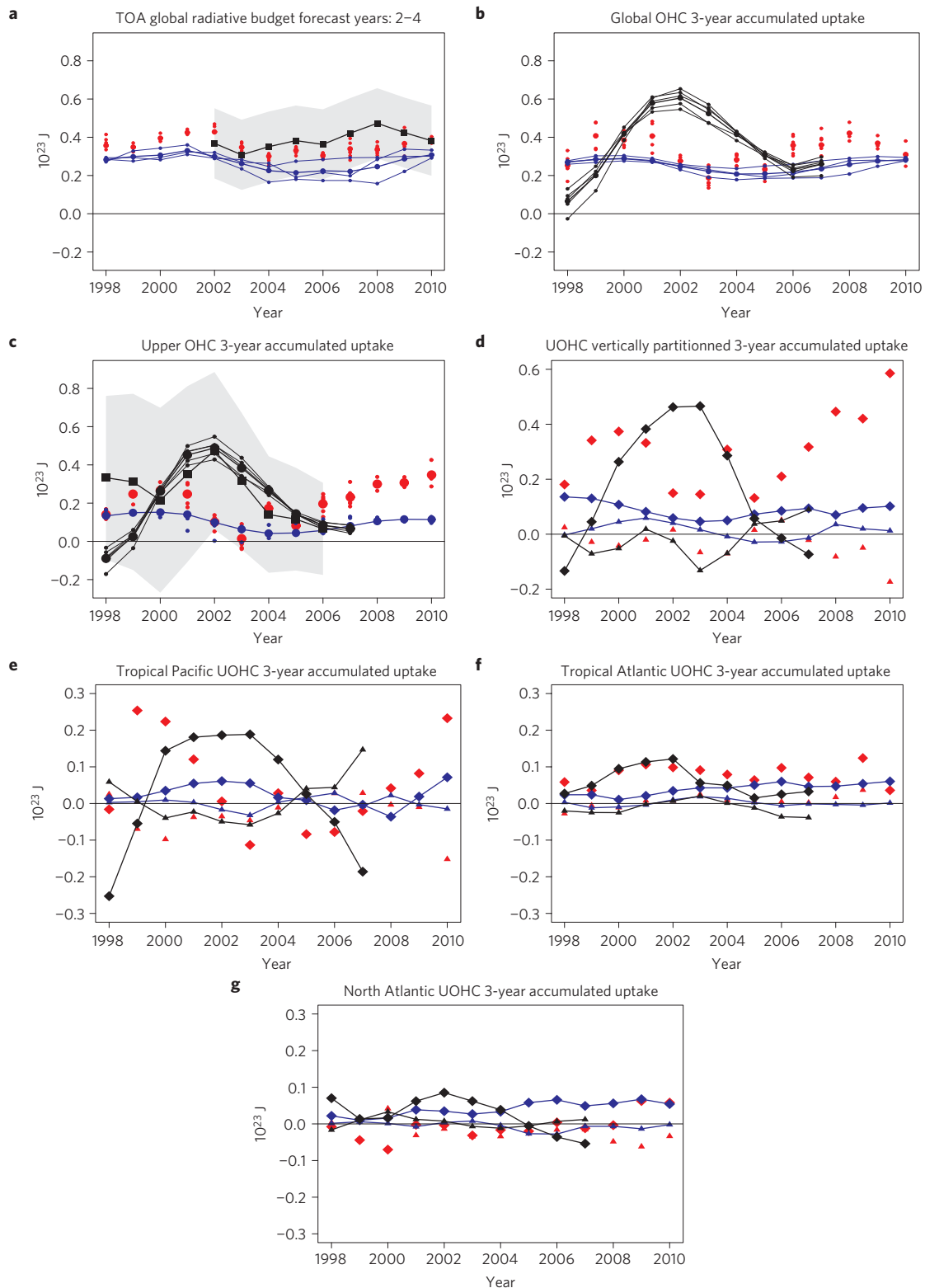
Figure 2 | Earth's heat budget. a–g, Init, NoInit and the observational data are shown in red, blue and black, respectively. In **a–c**, one large symbol shows the ensemble mean, and small symbols show the individual members. Observations from CERES (**a**) and ref. 21 (0–700 m) (**c**) are shown with squares, with their observational uncertainty[19,21] shaded in grey. ORAS4 (ocean reanalysis) is shown with dots (**b–c**), triangles and diamonds (**d–g**). The contribution from the total column (**b**) and from the total 0–724 m layer (**c**), are shown with dots for ORAS4, Init and NoInit. In **d–g**, the contribution from the ocean mixed layer and from the 0–724 m layer excluding the mixed layer are shown respectively with triangles and diamonds.

Fig. S6), but not by NoInit (Supplementary Fig. S7). The Init tropical Atlantic OHC tendency follows the ORAS4 one closely (Fig. 2f). However, the North Atlantic peak is completely missed by Init (Fig. 2g), hence its underestimation of the total-column ocean

heat uptake (Fig. 2b) and SST tendency (Fig. 1d). The benefits from the initialization in capturing the spatial distribution of the ocean heat uptake during the onset of the warming pause are further illustrated in Supplementary Fig. S8.
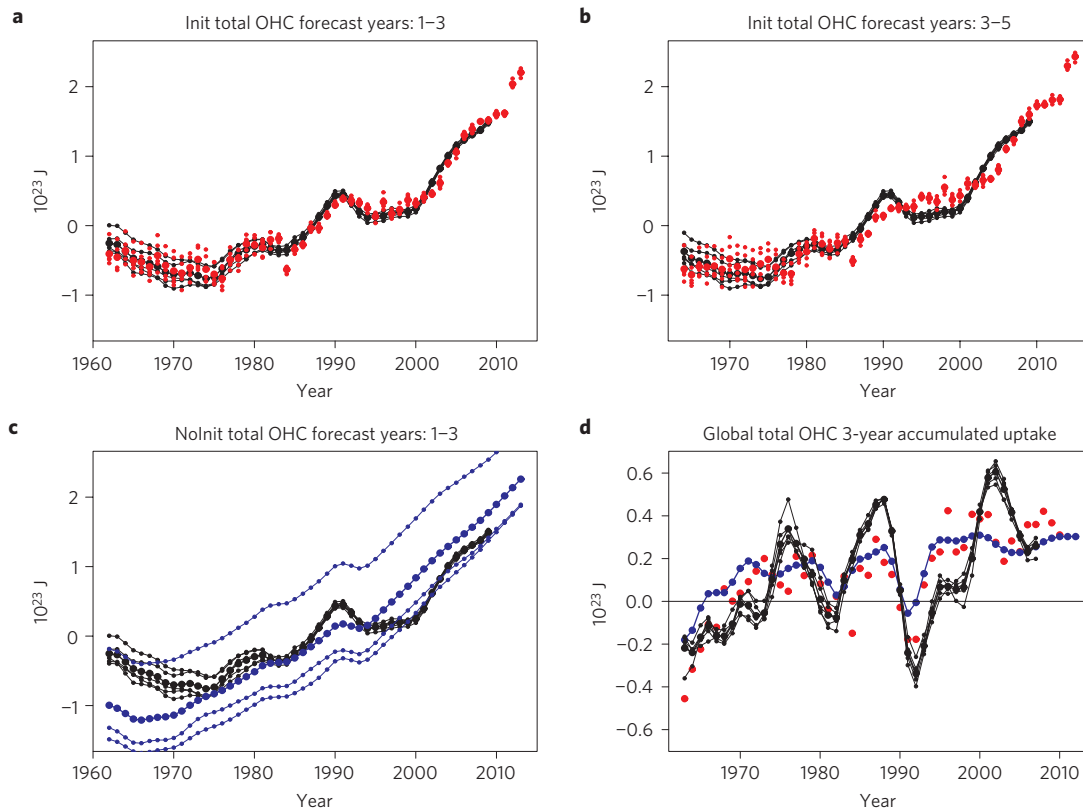
Figure 3 | Ability to predict the ocean heat storage. a–c, Total global OHC anomalies averaged across forecast years 1–3 (**a,c**) and forecast years 3–5 (**b**). **d**, 3-year accumulated heat uptake along the forecasts. One large dot is shown for the ensemble mean of each forecast and small dots are shown for their members in Init (red). The equivalents in NoInit and in the ORAS4 reanalysis are shown in blue and black respectively, joined by lines as they come from a continuous time series.

Whereas some previous modelling studies[2,3] suggested an increase in deep-ocean heat uptake as the main cause for the recent hiatus, such a hypothesis does not explain the onset of the warming slowdown either in the ORAS4 reanalysis, or in the EC-Earth retrospective predictions. The deep-ocean heat uptake has been argued[4] to be largely overestimated by most climate models, which does not seem to be the case for EC-Earth, although the scarce observations do not constrain to firm conclusions about the deep ocean. Suggested contributions from the deep prolonged solar minimum[4], the stratospheric water vapour[5], the stratospheric[4,6] and tropospheric aerosols[7] would be associated with a decrease in the net TOA energy imbalance to produce a warming slowdown such as the one recently observed. Here, we have shown that the contribution from variations in the external radiative forcing to the onset of the hiatus is negligible and that the initialization of EC-Earth from estimates of the observed climate state is essential to capture this warming slowdown (Fig. 1). At the onset of the warming pause, the TOA excess energy input is mainly absorbed in the upper 700 m ocean below the ocean mixed layer (Fig. 2), which confirms a previous hypothesis[19] drawn from observational analyses. The reasons for the warming pause to be sustained late in the decade have not however been clearly identified from our experiments. This climate prediction exercise has thus allowed for an attribution of the onset of the hiatus to an enhanced ocean heat uptake.

Methods

The decadal predictions. The decadal integrations were performed with the EC-Earth version 2.3 coupled atmosphere–ocean general circulation model[13,14]. The 5-member ORAS4 ocean reanalysis[15,16] provided the five different ocean initial conditions. The atmosphere and land surface ones were taken from the

ERA-40 reanalysis[17] before 1989 and the ERA-Interim one[18] afterwards. Singular vectors were applied to obtain atmospheric initial perturbations. The greenhouse gases, solar cycle and aerosol concentrations follow the CMIP5 (Fifth Coupled Model Intercomparison Project) recommendations[22]. We use two sets of decadal predictions: the first one consists of 10-year-long 5-member hindcasts initialized in November every year over the period 1960–2005. This ensemble is referred to as Init1. The sea-ice initial conditions were issued from a NEMO2/LIM2 simulation forced with DFS4.3 (ref. 23). The second set consists of 10-year long 3-member hindcasts initialized every November over the period 2001–2011. The sea-ice initial conditions came from the GLORYS2V1 reanalysis. This ensemble is referred to as Init2. For the sake of figure clarity, Init1 and Init2 are used as a single ensemble experiment, referred to as Init. We also use a 3-member sister ensemble that has been built from the historical simulations and the first years of the climate change projections following the Representative Concentration Pathway 4.5 scenario[22]. This ensemble is referred to as NoInit.

The observational data sets. The validation of those decadal integrations relies on the following observational data sets, SST: the NOAA Extended Reconstructed SST v3b data set[24] (named ERSST); sea-ice concentration: the NSIDC (ref. 25; updated to 2008) and the HadISST v1.1 data sets[26] (named HadISST); TOA radiative fluxes: the CERES EBAF-TOA Ed2.6r data set[27] (named CERES); OHC: the ORAS4 (refs 15,16), the GLORYS2v1 (ref. 28) and the Ishii and Kimoto[29] reanalyses.

Computation of the anomalies. For each variable, the baseline period selected to compute the model and observation anomalies is the longest period covered entirely by the observations and by the same number of starting dates for all the forecast times. The model climatology is then defined as a function of forecast time, by averaging the forecast variable across the members and the starting dates, using only forecast values that lie in the baseline period. For example, if an observational data set covers the January 1850 to December 2012 period, the baseline period selected from the temporal coverage of Init1, NoInit and this observational data set is November 1969 to October 2006. The starting dates from 1969–2005 will be used to compute the model climatology for forecast year 1, 1968–2004 for forecast year 2, and so on, until 1960–1996 for forecast year 10. This methodology allows the anomalies at different forecast times to be relative to the exact same baseline period, and the observation climatology does not depend on the forecast year. The

model climatologies obtained in such a way are then subtracted from each raw retrospective forecast to obtain anomalies over the whole forecasted period. As the Init2 set of forecasts is shorter, the climatology computed for Init1 is used for Init2 after an adjustment by the difference in climatology between Init2 and Init1 over the 2001–2005 set of forecasts. Drift-correcting any variable consists of adding the observed climatology to the modelled anomalies. For the TOA radiative fluxes, as the CERES observational data set covers only the twenty-first century and as we aim at assessing whether the net TOA imbalance is biased in EC-Earth as compared with the CERES data over this short period, the Init TOA radiative fluxes have been drift-corrected by using NoInit as equivalent observations instead of the CERES data. We therefore allow Init to have the same mean bias as NoInit over their common period but we remove the drift in Init. This ensures independent drift-correction and bias validation against the CERES data.

Computation of the 3-year accumulated heat uptake and 3-year SST change.
The ability of EC-Earth to reproduce the mechanisms leading to the warming slowdown is investigated by validating the tendencies along the forecasts. The 3-year mean change in a variable X computed by subtracting the observed X anomaly at the initialization date from the predicted X anomaly at forecast year 3 is noisy. To reduce this noise, we use the 3-year average predicted X anomaly at forecast time 3–5 years from which we subtract the 3-year average observed X anomaly around the initialization date, from the year before initialization to forecast year 2. The 3-year tendency in NoInit is computed by subtracting the simulated X anomaly averaged across the equivalent forecast times $(-1) - 2$ years to the simulated X anomaly averaged across the equivalent forecast times 3–5 years. To compute the 3-year accumulated heat uptake in various regions, we define the tropical band as encompassing 30° S–30° N, and the North Atlantic, North Pacific, Arctic and Antarctic regions as covering, respectively, 10°–65° N, 10°–70° N, 65°–90° N and 90°–60° S.

References

1. Knight, J. Global oceans: Do global temperature trends over the last decade falsify climate predictions? *Bull. Am. Meteorol. Soc.* **90,** S56–S57 (2009).
2. Katsman, C. A. & van Oldenborgh, G. J. Tracing the upper ocean's missing heat. *Geophys. Res. Lett.* **38,** L14610 (2011).
3. Meehl, G. A., Arblaster, J. M., Fasullo, J. Y., Hu, A. & Trenberth, K. E. Model-based evidence of deep-ocean heat uptake during surface-temperature hiatus periods. *Nature Clim. Change* **1,** 360–364 (2011).
4. Hansen, J., Sato, M., Kharecha, P. & von Schuckmann, K. Earth's energy imbalance and implications. *Atmos. Chem. Phys.* **11,** 13421–13449 (2011).
5. Solomon, S. Contributions of stratospheric water vapor to decadal changes in the rate of global warming. *Science* **327,** 1219–1223 (2010).
6. Solomon, S. The persistently variable 'background' stratospheric aerosol layer and global climate change. *Science* **333,** 866–870 (2011).
7. Kaufmann, R. K., Kauppib, H., Mann, M. L. & Stock, J. H. Reconciling anthropogenic climate change with observed temperature 1998–2008. *Proc. Natl Acad. Sci. USA* **108,** 790–793 (2011).
8. Trenberth, K. E. & Fasullo, J. T. Tracking earth's energy. *Science* **328,** 316–317 (2010).
9. Smith, D. *et al.* Improved surface temperature prediction for the coming decade from a global climate model. *Science* **317,** 796–799 (2007).
10. Keenlyside, N. S., Latif, M., Jungclaus, J., Kornblueth, L. & Roeckner, E. Advancing decadal-scale climate prediction in the North Atlantic sector. *Nature* **453,** 84–88 (2008).
11. Pohlmann, H., Jungclaus, J. H., Kohl, A., Stammer, D. & Marotzke, J. Initializing decadal climate predictions with the GECCO oceanic synthesis: Effects on the North Atlantic. *J. Clim.* **22,** 3926–3938 (2009).
12. Hawkins, E. & Sutton, R. The potential to narrow uncertainty in regional climate predictions. *Bull. Am. Meteorol. Soc.* **90,** 1095–1107 (2009).
13. Hazeleger, W. *et al.* EC-Earth V2.2: Description and validation of a new seamless Earth system prediction model. *Clim. Dyn.* **39,** 2611–2629 (2012).
14. Du, H. *et al.* Sensitivity of decadal predictions to the initial atmospheric and oceanic perturbations. *Clim. Dyn.* **39,** 2013–2023 (2012).
15. Mogensen, K. S., Balmaseda, M. A. & Weaver, A. T. *The NEMOVAR Ocean Data Assimilation As Implemented in the ECMWF Ocean Analysis for System 4* Technical Memorandum 668 (ECMWF, 2011).
16. Balmaseda, M. A., Mogensen, K. S. & Weaver, A. T. Evaluation of the ECMWF ocean reanalysis ORAS4. *Q. J. R. Meteorol. Soc.* http://dx.doi.org/10.1002/qj.2063 (2012).
17. Uppala, S *et al.* ERA-40: ECMWF 45-year reanalysis of the global atmosphere and surface conditions 1957–2000. *ECMWF Newsl.* **101,** 2–21 (2004).
18. Dee, D. P. *et al.* The era-interim reanalysis: Configuration and performance of the data assimilation system. *Q. J. R. Meteorol. Soc.* **137,** 553–597 (2011).
19. Loeb, N. G. *et al.* Observed changes in the top-of-atmosphere radiation and upper-ocean heating consistent within uncertainty. *Nature Geosci.* **5,** 110–113 (2012).
20. Trenberth, K. E., Fasullo, J. T. & Kiehl, J. Earth's global energy budget. *Bull. Am. Meteorol. Soc.* **90,** 311–329 (2009).
21. Lyman, J. M. *et al.* Robust warming of the global upper ocean. *Nature* **465,** 334–337 (2010).
22. Taylor, K. E., Stouffer, R. J. & Meehl, G. A. An overview of CMIP5 and the experimental design. *Bull. Am. Meteorol. Soc.* **93,** 485–498 (2012).
23. Brodeau, L., Barnier, B., Treguier, A. M., Penduff, T. & Gulev, S. An ERA40-based atmospheric forcing for global ocean circulation models. *Ocean Model.* **31,** 88–104 (2009).
24. Smith, T. M., Reynolds, R. W. & Lawrimore, T. C. P. H. Improvements to NOAAs historical merged land-ocean surface temperature analysis (1880–2006). *J. Clim.* **21,** 2283–2296 (2008).
25. Meier, W., Fetterer, F., Knowles, K., Savoie, M. & Brodzik, M. J. *Sea Ice Concentrations From Nimbus-7 SMMR And DMSP SSM/I Passive Microwave Data* (National Snow and Ice Data Center, 2006).
26. Rayner, N. A. *et al.* Global analyses of sea surface temperature, sea ice, and night marine air temperature since the late nineteenth century. *J. Geophys. Res.* **108,** 1984–2012 (2003).
27. Loeb, N. G. *et al.* Toward optimal closure of the earth's top-of-atmosphere radiation budget. *J. Clim.* **22,** 748–766 (2009).
28. Ferry, N. *et al.* Mercator global Eddy permitting ocean reanalysis GLORYS1V1: Description and results. *Mercator Ocean Quart. Newsl.* **36,** 15–27 (2010).
29. Ishii, M. & Kimoto, M. Reevaluation of historical ocean heat content variations with time-varying XBT and MBT depth bias corrections. *J. Oceanogr.* **65,** 287–299 (2009).

Author contributions

V.G. and F.J.D-R. designed the research and performed the analyses. M.A. ran the experiments. V.G., F.J.D-R. and I.A-B. interpreted the results and wrote the article.

Additional information

Supplementary information is available in the online version of the paper. Reprints and permissions information is available online at www.nature.com/reprints. Correspondence and requests for materials should be addressed to V.G.

Competing financial interests

The authors declare no competing financial interests.